

Compressed Sensing Inspired User Acquisition for Downlink Integrated Sensing and Communication Transmissions

Yi Song^{*}, Fernando Pedraza^{*}, Shuangyang Li^{*}, Siyao Li^{*‡}, Han Yu[†], and
Giuseppe Caire^{*} ^{*}Faculty of Electrical Engineering and Computer Science,
Technical University of Berlin, Berlin, Germany [†]Department of Electrical
Engineering, Chalmers University of Technology, Gothenburg, Sweden
[‡]Department of Electrical Engineering, University of Alaska Anchorage, USA
E-mail: {yi.song, f.pedrazaniето, shuangyang.li, siyao.li, caire}@tu-berlin.de,
yuha@chalmers.se

Abstract

This paper investigates radar-assisted user acquisition for downlink multi-user multiple-input multiple-output (MIMO) transmission using Orthogonal Frequency Division Multiplexing (OFDM) signals. Specifically, we formulate a concise mathematical model for the user acquisition problem, where each user is characterized by its delay and beamspace response. Therefore, we propose a two-stage method for user acquisition, where the Multiple Signal Classification (MUSIC) algorithm is adopted for delay estimation, and then a least absolute shrinkage and selection operator (LASSO) is applied for estimating the user response in the beamspace. Furthermore, we also provide a comprehensive performance analysis of the considered problem based on the pair-wise error probability (PEP). Particularly, we show that the rank and the geometric mean of non-zero eigenvalues of the squared beamspace difference matrix determines the user acquisition performance. More importantly, we reveal that simultaneously probing multiple beams outperforms concentrating power on a specific beam direction in each time slot under the power constraint, when only limited OFDM symbols are transmitted. Our numerical results confirm our conclusions and also demonstrate a promising acquisition performance of the proposed two-stage

method.

I. INTRODUCTION

Integrated sensing and communications (ISAC) has recently received significant attention as a key enabling technology for future wireless networks [1], [2]. Specifically, ISAC achieves both communication and radar functionalities using the same equipment, spectrum, and signals, which enjoys lower costs, higher spectral efficiency, and higher energy efficiency compared to counterparts that require dedicated transceiver designs [3]–[8].

In modern communication systems, the demand for enhanced performance and efficiency has driven the exploration of innovative techniques to optimize user acquisition processes [9]. Conventional user acquisition schemes usually rely on the confirmation message sent from the user side [10]. However, thanks to the advancement of ISAC, it has been evident that user acquisition can be simplified to a target detection problem solvable by using the radar functionality, which does not require the dedicated confirmation message [11].

In this paper, we focus on the radar-assisted user acquisition for downlink multiple-input multiple output (MIMO) transmissions, where a base station (BS) broadcasts orthogonal frequency division multiplexing (OFDM) signals in the cell for detecting potential users. Notice that the radar target detection based on OFDM signals is not straightforward due to the inevitable superposition among the backscattered signals from different targets and the potential frequency selectivity. Conventional methods for such a problem may rely on the matched filtering that examines all possible combinations of delay and beamspace with a dedicated resolution [12], which inevitably introduces a high complexity. Hence, we are motivated to consider compressed sensing-type algorithms by noticing that the number of users is generally smaller than the size of the beamspace in a massive MIMO (mMIMO) setup.

The work of Fernando Pedraza, Shuangyang Li, and Giuseppe Caire was supported in part by BMBF Germany in the program of “Souverän. Digital. Vernetzt.” Joint Project 6G-RIC (Project IDs 16KISK030). In addition, the work of Shuangyang Li was also supported in part by the European Union’s Horizon 2020 Research and Innovation Program under MSCA Grant No. 101105732 – DDComRad. The work of Siyao Li was partially funded by the European Research Council under the ERC Advanced Grant N. 789190, CARENET. The work of Han Yu is supported in part by European Commission 101095759 Hexa-X-II.

Indeed, compressed sensing (CS) algorithms have been explored in the context of downlink frequency-division duplex (FDD) mMIMO systems for channel estimation. For instance, in [13], the authors capitalize on the spatial sparsity of users' channels using discrete fourier transform (DFT) matrices and subsequently employ the joint orthogonal matching pursuit (JOMP) algorithm for estimating user responses in the angular domain. However, this approach is constrained to single carrier waveforms and lacks direct extension to the OFDM case. Another consideration is the orthogonal matching pursuit (OMP) algorithm in the multi-carrier system, as discussed in [14], where joint estimation of angle and delay coefficients is performed. Unfortunately, this method relies on fine resolution of angle-delay grids, potentially leading to high computational complexity in practical applications.

Against this background, we propose a novel two-stage algorithm in this paper by exploiting the user sparsity in the beamspace. Specifically, the proposed algorithm employs the multiple signal classification (MUSIC) algorithm for delay estimation, followed by a least absolute shrinkage and selection operator (LASSO) for beamspace matrix estimation. Such a scheme decouples the impact of delay from the beamspace coefficient estimation and exploits the sparsity. Furthermore, we conduct a comprehensive theoretical performance analysis utilizing pairwise error probability (PEP), and demonstrate that the rank of the squared beamspace difference matrix determines the error exponent, while the geometric mean of its non-zero eigenvalues characterizes the potential signal-to-noise ratio (SNR) improvements. Based to the PEP analysis, we reveal that probing multi-beams to different directions simultaneously generally requires less time to have a good acquisition performance compared to the conventional beam sweeping strategy, i.e., single beam at each time slot, under the same power constraint. However, as the number of time slots increases sufficiently, the beam sweeping strategy shall present a better performance. Numerical results confirm our conclusions from the PEP analysis and also validate the effectiveness of the proposed two-stage method.

Notations: The superscripts $(\cdot)^H$ and $(\cdot)^T$ denote the Hermitian transpose and transpose of a matrix, respectively; $f^*(\cdot)$ and $\text{vec}(\cdot)$ denote the conjugate of $f(\cdot)$ and the vectorization of a matrix; $\text{Unif}[x, y]$ denotes the uniform distribution from x to y ; \mathbf{I} represents the identity matrix; $\mathbb{E}[\cdot]$ denotes the statistical expectation.

II. SYSTEM MODEL

We focus on the downlink ISAC transmission utilizing OFDM signaling, functioning at a carrier frequency f_c . We assume that the occupied bandwidth is sufficiently smaller than f_c such that the narrow-band array response assumption holds. Furthermore, we consider the case where the transmitter array and radar receiver array are co-located with each other at the BS, and the transmitted and received signals are perfectly separable by advanced full-duplex processing. We assume that the BS is equipped with a uniform linear array (ULA) with M antenna elements connected to a single RF chain, and the targets are located in the far-field.

We consider the point target model, where the p -th target is sufficiently characterized by its line-of-sight (LoS) path with the angle of arrival (AoA) ϕ_p with the marginal Doppler effect after compensated. For a time-invariant backscatter channel with P separable targets¹, its impulse response is given by

$$\mathbf{H}(\tau) = \sum_{p=1}^P h_p \mathbf{a}(\phi_p) \mathbf{a}^H(\phi_p) \delta(\tau - \tau_p), \quad (1)$$

where for each target p , h_p is a complex radar channel gain including the LoS path loss, and is assumed to be a zero mean circularly-symmetric complex Gaussian variable with variance $C_{h_p} \triangleq \mathbb{E}[|h_p|^2] = \frac{\lambda^2 \sigma_{p,\text{rCS}}}{(4\pi)^3 d_p^4}$ [15], where λ is the signal wavelength, $\sigma_{p,\text{rCS}}$ is the radar cross section (RCS) and d_p is the relative distance between the p -th target and the BS. Moreover, $\tau_p = \frac{2d_p}{c}$ is the round-trip delay (time of flight), where c denotes the speed of light, and ϕ_p is the AoA. In (1), $\mathbf{a}(\phi_p)$ is the array response vector of length M , whose i -th element is given by $[\mathbf{a}(\phi_p)]_i = e^{j\pi(i-1)\sin(\phi_p)}$, $1 \leq i \leq M$.

A. OFDM Signaling for Target Detection

We focus on the signal transmission for the l -th OFDM symbol. Let $s_l(t)$ be the continuous-time OFDM transmitted signal without cyclic prefix (CP) at l -th time slot, which is written by $s_l(t) = \sum_{k=1}^{N_s} x_l[k] p(t - lT) e^{-j2\pi \frac{k-1}{T}(t-lT)}$, where T is the OFDM symbol duration, N_s is the number of subcarriers, $x_l[k]$ is the information symbol on the k -th subcarrier at the l -th time slot satisfying $\mathbb{E}[|x_l[k]|^2] = 1$, and $p(t)$ is the baseband shaping pulse. As the information symbols are placed in the frequency domain, we are interested in the frequency domain channel response

¹Here, we consider the channel from the BS transmitter to the BS radar receiver, reflected by the targets.

corresponding to (1). Notice that (1) is time-invariant. Therefore, the frequency domain channel matrix of size $M \times M$ is also time-invariant, which can be calculated by

$$\begin{aligned}\tilde{\mathbf{H}}_k &= \int_{-\infty}^{\infty} \mathbf{H}(\tau) e^{-j2\pi \frac{k-1}{T} \tau} d\tau \\ &= \sum_{p=1}^P h_p \mathbf{a}(\phi_p) \mathbf{a}^H(\phi_p) e^{-j2\pi \frac{k-1}{T} \tau_p}, \quad \forall k \in [N_s],\end{aligned}\quad (2)$$

where k is the subcarrier index. Thus, by transmitting OFDM signal $s_l(t)$ over the channel characterized by (1) with a sufficiently long CP, and considering the same beamforming vector \mathbf{v}_l is applied at the transmitter and the receiver, we can derive the frequency domain channel observations after the CP removal and matched-filtering as

$$y_l[k] = \mathbf{v}_l^H \tilde{\mathbf{H}}_k \mathbf{v}_l x_l[k] + n_l[k], \quad (3)$$

where $y_l[k]$ and $n_l[k]$ are the received symbol and the noise sample on the k -th subcarrier at the l -th time slot, respectively. We assume that the BS makes use of a beamforming codebook basis $\mathbf{F} = [\mathbf{f}_1, \mathbf{f}_2, \dots, \mathbf{f}_{N_b}]$ of cardinality N_b , where $N_b < M$. The adopted beamforming vectors are synthesized as a linear combination of the codebook entries, i.e.,

$$\mathbf{v}_l = \sum_{i=1}^{N_b} w_{l,i} \mathbf{f}_i, \quad (4)$$

where $0 \leq w_{l,i} \leq 1$ is the weight for the i -th beamformer \mathbf{f}_i at the l -th time slot. Focusing on codebooks with approximately pairwise orthonormal columns, i.e., $\mathbf{F}^H \mathbf{F} \approx \mathbf{I}$, we further constraint the weights to satisfy $\sum_{i=1}^{N_b} |w_{l,i}|^2 = 1$ such that $\|\mathbf{v}_l\|^2 = 1$. Specifically, we consider codebook vectors with approximately constant gain within their beamwidths and low gain elsewhere, designed as described in [16, App. A]. Furthermore, we construct the codebook such that each angle is covered by a single beam, i.e., $|\mathbf{f}_i^H \mathbf{a}(\phi)| \gg 1$ implies $|\mathbf{f}_j^H \mathbf{a}(\phi)| \approx 0$ for $i \neq j$. In such a case, the noise sample $z_l[k]$ is a zero mean complex Gaussian variable, i.e., $\mathbb{E}[n_l[k] n_l^*[k]] = N_0 \mathbf{v}_l^H \mathbf{v}_l = N_0$, where N_0 is the one-sided power spectral density of the underlying additive white Gaussian noise (AWGN) process.

By substituting (4) into (3), the received signal is given by

$$\begin{aligned}y_l[k] &= \mathbf{v}_l^H \tilde{\mathbf{H}}_k \mathbf{v}_l x_l[k] + n_l[k] \\ &= \sum_{i=1}^{N_b} \sum_{j=1}^{N_b} w_{l,i} w_{l,j}^* \mathbf{f}_j^H \tilde{\mathbf{H}}_k \mathbf{f}_i x_l[k] + n_l[k].\end{aligned}\quad (5)$$

For the k -th subcarrier, note that $|\mathbf{f}_j^H \mathbf{a}(\phi_p) \mathbf{a}^H(\phi_p) \mathbf{f}_i| \approx 0$ for $i \neq j$ and all ϕ_p holds due to the codebook. Hence, based on the definition of $\tilde{\mathbf{H}}_k$ in (2), (5) can be further simplified as $y_l[k] = \sum_{i=1}^{N_b} |w_{l,i}|^2 \mathbf{f}_i^H \tilde{\mathbf{H}}_k \mathbf{f}_i x_l[k] + n_l[k]$. Note that $x_l[k]$ as the pilot information is known at the radar receiver, so we are able to define the received signal as $r_l[k] \triangleq y_l[k]/x_l[k]$ and the effective noise as $z_l[k] \triangleq n_l[k]/x_l[k]$, and rewrite $y_l[k]$ based on the channel formulation in (2) as

$$\begin{aligned} r_l[k] &= \sum_{i=1}^{N_b} |w_{l,i}|^2 \mathbf{f}_i^H \tilde{\mathbf{H}}_k \mathbf{f}_i + z_l[k] \\ &= \sum_{i=1}^{N_b} \sum_{p=1}^P |w_{l,i}|^2 h_p e^{-j2\pi \frac{k-1}{T} \tau_p} \mathbf{f}_i^H \mathbf{a}(\phi_p) \mathbf{a}(\phi_p)^H \mathbf{f}_i + z_l[k] \end{aligned} \quad (6)$$

where $z_l[k]$ has the same variance of $n_l[k]$ for energy normalized $x_l[k]$. Furthermore, by stacking $r_l[k]$ for all $k \in [N_s]$ into a vector, the observations at the l -th time slot is given by

$$\begin{aligned} \mathbf{r}_l &= \begin{bmatrix} \sum_{i=1}^{N_b} \sum_{p=1}^P |w_{l,i}|^2 h_p \mathbf{f}_i^H \mathbf{a}(\phi_p) \mathbf{a}(\phi_p)^H \mathbf{f}_i \\ \sum_{i=1}^{N_b} \sum_{p=1}^P |w_{l,i}|^2 h_p e^{-j2\pi \frac{1}{T} \tau_p} \mathbf{f}_i^H \mathbf{a}(\phi_p) \mathbf{a}(\phi_p)^H \mathbf{f}_i \\ \vdots \\ \sum_{i=1}^{N_b} \sum_{p=1}^P |w_{l,i}|^2 h_p e^{-j2\pi \frac{N_s-1}{T} \tau_p} \mathbf{f}_i^H \mathbf{a}(\phi_p) \mathbf{a}(\phi_p)^H \mathbf{f}_i \end{bmatrix} \\ &+ [z_l[1], z_l[2], \dots, z_l[N_s]]^T \triangleq \mathbf{T} \mathbf{w}_l + \mathbf{z}_l, \end{aligned} \quad (7)$$

where for notational simplicity, we let

$$\mathbf{w}_l = [|w_{l,1}|^2, |w_{l,2}|^2, \dots, |w_{l,N_b}|^2]^T \quad (8)$$

as the *beam weight vector* for the l -th time slot, and let the effective noise vector as $\mathbf{z}_l = [z_l[1], \dots, z_l[N_s]]^T$. More importantly, we define $\mathbf{T} \in \mathbb{C}^{N_s \times N_b}$ as the *radar response matrix* and it can be decomposed as $\mathbf{T} = \sum_{p=1}^P h_p \mathbf{b}(\tau_p) \mathbf{q}_p^T$, where $\mathbf{b}(\tau_p)$ is the *delay steering vector* of length- N_s represented by $\mathbf{b}(\tau_p) \triangleq [1, e^{-j2\pi \frac{1}{T} \tau_p}, \dots, e^{-j2\pi \frac{N_s-1}{T} \tau_p}]^T$, and \mathbf{q}_p denotes the *target beamspace vector* of length- N_b characterizing the reflectivity of the p -th target with respect to each possible beam direction, given as $\mathbf{q}_p = [\mathbf{f}_1^H \mathbf{a}(\phi_p) \mathbf{a}^H(\phi_p) \mathbf{f}_1, \dots, \mathbf{f}_{N_b}^H \mathbf{a}(\phi_p) \mathbf{a}^H(\phi_p) \mathbf{f}_{N_b}]^T$. Since we could not decouple the effect of h_p for the user detection problem, we also define $\mathbf{g}_p \triangleq h_p \mathbf{q}_p$ and our goal is to estimate \mathbf{g}_p , which contains the information of the user location in the beamspace, based on the observations collected within the L time slots. If we stack the delay steering vectors for all delays as $\mathbf{B} \triangleq [\mathbf{b}(\tau_1), \dots, \mathbf{b}(\tau_P)] \in \mathbb{C}^{N_s \times P}$, and also stack \mathbf{g}_p for all

targets together as $\mathbf{G} \triangleq [\mathbf{g}_1, \dots, \mathbf{g}_P] \in \mathbb{C}^{N_b \times P}$, the radar response matrix \mathbf{T} can be reformulated as $\mathbf{T} = \mathbf{B}\mathbf{G}^T$.

B. Problem Formulation

Without loss of generality, let us consider the transmission for sensing purpose with L time slots. Define $\mathbf{R} \triangleq [\mathbf{r}_1, \mathbf{r}_2, \dots, \mathbf{r}_L] \in \mathbb{C}^{N_s \times L}$ the collection of the observation vectors at all time slots. Then, according to (7), and \mathbf{T} , the observation matrix for L time slots is given by

$$\mathbf{R} = \mathbf{T}\mathbf{W} + \mathbf{Z} = \sum_{p=1}^P \mathbf{b}(\tau_p) \mathbf{g}_p^T \mathbf{W} + \mathbf{Z} = \mathbf{B}\mathbf{G}^T \mathbf{W} + \mathbf{Z}. \quad (9)$$

where $\mathbf{W} = [\mathbf{w}_1, \dots, \mathbf{w}_L]$ is the *beam scheduling matrix* of size $N_b \times L$, whose l -th column is given by \mathbf{w}_l in (8), and $\mathbf{Z} \triangleq [\mathbf{z}_1, \mathbf{z}_2, \dots, \mathbf{z}_L]$ is the effective noise matrix. While systems of the type of (9) can be solved for \mathbf{G} under certain conditions given knowledge of \mathbf{B} and \mathbf{W} , the lack of knowledge about target delays prevents us from directly applying standard techniques. Nevertheless, we can exploit the structure of the matrices involved and propose an efficient method to estimate the nonzero entries of \mathbf{G} .

III. THE USER ACQUISITION METHOD

In this section, we introduce a two-stage user acquisition method to address the problem formulated in Section II. Specifically, the proposed method begins by estimating the delay using the MUSIC and subsequently employs a straightforward compressed sensing approach to detect all users in the beam space. Before introducing the details on the proposed methods, we first introduce two beam probing strategies, namely, the *beam sweeping strategy* and the *random multi-beam strategy*, focusing on the design of beam weight vectors across different time slots.

A. Beam Probing Strategies

1) *Beam sweeping strategy*: The beam sweeping strategy aims to probe the signals to all possible beam directions in a sequential manner across different time slots. Specifically, the beam weight vector at the l -th time slot can be expressed as follows, $\mathbf{w}_l^s = [0, \dots, 1, 0, \dots, 0]^T$, $\forall l \in [L]$, where the only l -th element of \mathbf{w}_l^s is set to 1, which indicates that we probe in the l -th beam direction at the l -th time slot. Such a beam probing strategy enables a sufficient power concentration towards the intended beam direction.

2) *Random multi-beam strategy*: In this strategy, instead of probing exclusively within a specific beam direction, we employ a random probing approach with \mathbf{w}_l^r , $\forall l \in [L]$, and each element of \mathbf{w}_l^r is given by $[\mathbf{w}_l^r]_i = \alpha \tilde{w}_{l,i}^2, \forall i \in [N_b]$, where $\tilde{w}_{l,i}$ is unit Gaussian distributed, i.e., $\tilde{w}_{l,i} \sim \mathcal{N}(0, 1)$. Moreover, the power scale factor is set as $\alpha = \frac{1}{N_b}$ to satisfy the constraint for the beam weight vector that $\mathbb{E} \left[\sum_{i=1}^{N_b} [\mathbf{w}_l^r]_i \right] \triangleq 1$. The aim for such a beam probing strategy is to spread the signal power towards many beam directions at the same time.

B. The Two-stage User Acquisition Method

We introduce the two-stage method for user acquisition in the beamspace based on the two proposed probing strategies.

1) *Stage I: delay estimation using the MUSIC algorithm for P targets*: Based on the formulation of the received signal in (9), assuming that the beam scheduling matrix \mathbf{W} and noise \mathbf{Z} are independent, the auto-correlation function of the received signal \mathbf{R} is calculated as

$$\begin{aligned} \mathbb{E}[\mathbf{R}\mathbf{R}^H] &= \mathbf{B}\mathbf{G}^T \mathbb{E}[\mathbf{W}\mathbf{W}^H] \mathbf{G}^* \mathbf{B}^H + \mathbb{E}[\mathbf{Z}\mathbf{Z}^H] \\ &\triangleq \mathbf{B}\mathbf{R}_s \mathbf{B}^H + LN_0 \mathbf{I}, \end{aligned} \quad (10)$$

where \mathbf{R}_s is a matrix with size $P \times P$, defined as $\mathbf{R}_s \triangleq \mathbf{G}^T \mathbb{E}[\mathbf{W}\mathbf{W}^H] \mathbf{G}^*$. In addition, $\mathbf{B} \triangleq [\mathbf{b}(\tau_1), \dots, \mathbf{b}(\tau_P)]$ is a Vandermonde matrix with size $N_s \times P$. The form of $\mathbb{E}[\mathbf{R}\mathbf{R}^H]$ in (10) allows for the use of the MUSIC algorithm to estimate the delays $\tau_p, \forall p \in [P]$ using the eigenspace method. However, the auto-correlation function of \mathbf{R} is not known in advance. It can be estimated by using the samples collected over L times slots, $\hat{\mathbf{C}}_{\mathbf{R}} = \mathbf{R}\mathbf{R}^H$. Since $\hat{\mathbf{C}}_{\mathbf{R}} \in \mathbb{C}^{N_s \times N_s}$ is a Hermitian matrix, the eigenvalue decomposition on $\hat{\mathbf{C}}_{\mathbf{R}}$ is denoted as $\hat{\mathbf{U}} \hat{\mathbf{\Lambda}} \hat{\mathbf{U}}^H$ with decreasing order on the eigenvalues, i.e., $\hat{\mathbf{\Lambda}} = \text{diag}(\hat{\lambda}_1, \dots, \hat{\lambda}_{N_s})$ and $\hat{\lambda}_1 \geq \hat{\lambda}_2 \geq \dots \geq \hat{\lambda}_{N_s}$, and all of its eigenvectors $\hat{\mathbf{U}} = [\hat{\mathbf{u}}_1, \dots, \hat{\mathbf{u}}_{N_s}]$ are orthogonal. The eigenvectors corresponding to the P largest eigenvalues span the signal subspace \mathcal{P}_S , while the rest of the eigenvectors span the noise space \mathcal{P}_N . Those two subspaces are orthogonal, i.e., $\mathcal{P}_S \perp \mathcal{P}_N$. By exploiting the orthogonal subspaces, the pseudo-spectrum for the delay τ is defined as

$$P_{\text{MU}}(\tau) = \|\mathbf{b}(\tau)^H \hat{\mathbf{U}}_N\|^2, \quad \forall 0 \leq \tau \leq T, \quad (11)$$

where $\hat{\mathbf{U}}_N \triangleq [\hat{\mathbf{u}}_{P+1}, \dots, \hat{\mathbf{u}}_{N_s}]$ denotes the eigenvectors of the noise subspace. Then the MUSIC algorithm can estimate the delays $\{\hat{\tau}_1, \dots, \hat{\tau}_P\}$ by identifying P dominant minimizers of the pseudo-spectrum $P_{\text{MU}}(\tau)$.

2) *Stage II: beamspace estimation using the LASSO algorithm:* After applying the MUSIC algorithm on the received signals, the delay estimation for P targets can be obtained as $\hat{\boldsymbol{\tau}} = [\hat{\tau}_1, \dots, \hat{\tau}_P]$. Hence, the delay steering vectors based on delay estimates can be reconstructed as $\hat{\mathbf{B}} = [\mathbf{b}(\hat{\tau}_1), \dots, \mathbf{b}(\hat{\tau}_P)]$. According to (9), the received signal in (9) can be reformulated as $\mathbf{R} \approx \hat{\mathbf{B}}\mathbf{G}^T\mathbf{W} + \mathbf{Z}$, which can be rewritten in vectorized form as

$$\text{vec}(\mathbf{R}) \approx (\mathbf{W}^T \otimes \hat{\mathbf{B}})\text{vec}(\mathbf{G}^T) + \text{vec}(\mathbf{Z}), \quad (12)$$

lying in the type of the compressive sensing problem. Then the beam space information \mathbf{G} can be estimated using the LASSO, given as

$$\min_{\mathbf{g}} \|\text{vec}(\mathbf{R}) - (\mathbf{W}^T \otimes \hat{\mathbf{B}})\mathbf{g}\|_2^2 + \beta\|\mathbf{g}\|_1, \quad (13)$$

where β is a regularization parameter controlling the sparsity of the solution and we have defined $\mathbf{g} \triangleq \text{vec}(\mathbf{G}^T)$. In particular, we solve (13) for different values of β and among the P -sparse solutions we choose the one which minimizes the reconstruction error. Let $\hat{\mathbf{G}} \in \mathbb{C}^{P \times N_b}$ denote the estimate beamspace matrix from (13), and thus for the p -th target corresponding to the estimate delay $\hat{\tau}_p$ from the MUSIC algorithm in (11), the estimate beam index of this target is given by $b_p^{\text{index}} = \arg \max_{i \in [N_b]} |[\hat{\mathbf{G}}]_{p,i}|^2$.

IV. PERFORMANCE ANALYSIS USING PAIRWISE ERROR PROBABILITY

To evaluate the accuracy of the proposed method, we employ the PEP framework to study the theoretical error performance. The PEP quantifies the probability of incorrectly detecting the variable of interest by its distorted version, which provides valuable insights for the design of beam probing strategies. This analysis also assumes the genie-aided delay estimation, i.e., the delays $\boldsymbol{\tau}$ are presumed to be known in advance. According to (9), the vectorization of \mathbf{R} can be reformulated as

$$\text{vec}(\mathbf{R}) = \begin{bmatrix} \mathbf{b}(\tau_1)\mathbf{q}_1^T\mathbf{w}_1 & \cdots & \mathbf{b}(\tau_P)\mathbf{q}_P^T\mathbf{w}_1 \\ \mathbf{b}(\tau_1)\mathbf{q}_1^T\mathbf{w}_2 & \cdots & \mathbf{b}(\tau_P)\mathbf{q}_P^T\mathbf{w}_2 \\ \vdots & & \vdots \\ \mathbf{b}(\tau_1)\mathbf{q}_1^T\mathbf{w}_L & \cdots & \mathbf{b}(\tau_P)\mathbf{q}_P^T\mathbf{w}_L \end{bmatrix} v + \begin{bmatrix} h_1 \\ h_2 \\ \vdots \\ h_P \end{bmatrix} + \begin{bmatrix} \mathbf{z}_1 \\ \mathbf{z}_2 \\ \vdots \\ \mathbf{z}_L \end{bmatrix} \triangleq \mathbf{D}_{\boldsymbol{\tau}, \mathbf{w}}(\mathbf{q})\mathbf{h} + \mathbf{z}, \quad (14)$$

where we define $\text{vec}(\mathbf{Z})$ as \mathbf{z} , and the matrix $\mathbf{D}_{\boldsymbol{\tau}, \mathbf{W}}(\mathbf{q})$ is a function of the beamspace vector \mathbf{q} depending on the delays $\boldsymbol{\tau}$ and the beam scheduling matrix \mathbf{W} . For a given channel realization and beam scheduling, let $\hat{\mathbf{q}}$ denote the estimate beamspace vector. By noticing that $\mathbf{h} \sim \mathcal{CN}(\mathbf{0}, \boldsymbol{\Lambda}_{\mathbf{h}})$, where $\boldsymbol{\Lambda}_{\mathbf{h}}$ is a diagonal matrix with its i -th diagonal element as $\mathbb{E}[|h_i|^2]$, $\forall i \in [P]$, we shall define the conditional Euclidean distance $d_{\mathbf{h}, \boldsymbol{\tau}, \mathbf{W}}^2(\mathbf{q}, \hat{\mathbf{q}})$ between the true \mathbf{q} and estimate beamspace vector $\hat{\mathbf{q}}$ as

$$\begin{aligned}
d_{\mathbf{h}, \boldsymbol{\tau}, \mathbf{W}}^2(\mathbf{q}, \hat{\mathbf{q}}) &\triangleq \|(\mathbf{D}_{\boldsymbol{\tau}, \mathbf{W}}(\mathbf{q}) - \mathbf{D}_{\boldsymbol{\tau}, \mathbf{W}}(\hat{\mathbf{q}})) \mathbf{h}\|^2 \\
&= \mathbf{h}^{\text{H}} (\mathbf{D}_{\boldsymbol{\tau}, \mathbf{W}}(\mathbf{q}) - \mathbf{D}_{\boldsymbol{\tau}, \mathbf{W}}(\hat{\mathbf{q}}))^{\text{H}} \underbrace{(\mathbf{D}_{\boldsymbol{\tau}, \mathbf{W}}(\mathbf{q}) - \mathbf{D}_{\boldsymbol{\tau}, \mathbf{W}}(\hat{\mathbf{q}}))}_{\tilde{\mathbf{D}}_{\boldsymbol{\tau}, \mathbf{W}}(\mathbf{E})} \mathbf{h} \\
&= \underbrace{(\boldsymbol{\Lambda}_{\mathbf{h}}^{-1/2} \mathbf{h})^{\text{H}}}_{\hat{\mathbf{h}}} \underbrace{\left(\boldsymbol{\Lambda}_{\mathbf{h}}^{1/2} \tilde{\mathbf{D}}_{\boldsymbol{\tau}, \mathbf{W}}(\mathbf{E})^{\text{H}} \tilde{\mathbf{D}}_{\boldsymbol{\tau}, \mathbf{W}}(\mathbf{E}) \boldsymbol{\Lambda}_{\mathbf{h}}^{1/2} \right)}_{\mathbf{P}_{\boldsymbol{\tau}, \mathbf{W}}(\mathbf{q}, \hat{\mathbf{q}})} \boldsymbol{\Lambda}_{\mathbf{h}}^{-1/2} \mathbf{h} \\
&= \hat{\mathbf{h}}^{\text{H}} \mathbf{P}_{\boldsymbol{\tau}, \mathbf{W}}(\mathbf{q}, \hat{\mathbf{q}}) \hat{\mathbf{h}}
\end{aligned} \tag{15}$$

where we define $\tilde{\mathbf{D}}_{\boldsymbol{\tau}, \mathbf{W}}(\mathbf{E}) \in \mathbb{C}^{LN_s \times P} \triangleq (\mathbf{D}_{\boldsymbol{\tau}, \mathbf{W}}(\mathbf{q}) - \mathbf{D}_{\boldsymbol{\tau}, \mathbf{W}}(\hat{\mathbf{q}}))$ corresponding to the detection difference matrix $\mathbf{E} = [\mathbf{e}_1, \dots, \mathbf{e}_P]$ with $\mathbf{e}_p = \mathbf{q}_p - \hat{\mathbf{q}}_p$, $\forall p \in [P]$. Let us further define the *squared beamspace difference matrix* $\mathbf{P}_{\boldsymbol{\tau}, \mathbf{W}}(\mathbf{q}, \hat{\mathbf{q}}) \triangleq \boldsymbol{\Lambda}_{\mathbf{h}}^{1/2} \tilde{\mathbf{D}}_{\boldsymbol{\tau}, \mathbf{W}}(\mathbf{E})^{\text{H}} \tilde{\mathbf{D}}_{\boldsymbol{\tau}, \mathbf{W}}(\mathbf{E}) \boldsymbol{\Lambda}_{\mathbf{h}}^{1/2}$, and $\hat{\mathbf{h}} \triangleq \boldsymbol{\Lambda}_{\mathbf{h}}^{-1/2} \mathbf{h}$, which satisfies $\hat{\mathbf{h}} \sim \mathcal{CN}(\mathbf{0}, \mathbf{I}_P)$. Since $\mathbf{z} \sim \mathcal{CN}(\mathbf{0}, N_0 \mathbf{I})$, the PEP is upper-bounded by [17] $\Pr(\mathbf{q} \rightarrow \hat{\mathbf{q}} | \hat{\mathbf{h}}, \boldsymbol{\tau}, \mathbf{W}) \leq \exp\left(-\frac{1}{4N_0} d_{\mathbf{h}, \boldsymbol{\tau}, \mathbf{W}}^2(\mathbf{q}, \hat{\mathbf{q}})\right)$. Assuming that the rank of $\mathbf{P}_{\boldsymbol{\tau}, \mathbf{W}}(\mathbf{q}, \hat{\mathbf{q}})$ is r and $r \leq \min\{LN_s, P\}$, let the eigenvalue decomposition on $\mathbf{P}_{\boldsymbol{\tau}, \mathbf{W}}(\mathbf{q}, \hat{\mathbf{q}})$ define as $\mathbf{U} \boldsymbol{\Lambda} \mathbf{U}^{\text{H}}$, where $\mathbf{U} = [\mathbf{u}_1, \dots, \mathbf{u}_P]$ denotes the eigenvectors and the corresponding eigenvalues are denoted as the diagonal elements of $\boldsymbol{\Lambda}$, i.e., $\boldsymbol{\Lambda} = \text{diag}(\lambda_1, \dots, \lambda_P)$. Note that all the eigenvalues are non-negative since $\mathbf{P}_{\boldsymbol{\tau}, \mathbf{W}}(\mathbf{q}, \hat{\mathbf{q}})$ is a positive semi-definite matrix. Therefore, the PEP can be reformulated as

$$\begin{aligned}
\Pr(\mathbf{q} \rightarrow \hat{\mathbf{q}} | \hat{\mathbf{h}}, \boldsymbol{\tau}, \mathbf{W}) &\leq \exp\left(-\frac{1}{4N_0} \hat{\mathbf{h}}^{\text{H}} \left(\sum_{p=1}^r \lambda_p \mathbf{u}_p \mathbf{u}_p^{\text{H}}\right) \hat{\mathbf{h}}\right) \\
&= \exp\left(-\frac{1}{4N_0} \sum_{p=1}^r \lambda_p |\tilde{h}_p|^2\right),
\end{aligned} \tag{16}$$

where $\tilde{h}_p \triangleq \mathbf{u}_p^{\text{H}} \hat{\mathbf{h}}$, $\forall p \in [P]$. It can be shown that $\{\tilde{h}_1, \dots, \tilde{h}_P\}$ are independent complex Gaussian random variables (RVs) with mean $\mu_{\tilde{h}_p} = \mathbf{u}_p^{\text{H}} \mathbb{E}[\mathbf{h}] = 0$ and variance $C_{\tilde{h}_p} = \mathbf{u}_p^{\text{H}} \mathbb{E}[\mathbf{h} \mathbf{h}^{\text{H}}] \mathbf{u}_p = 1$. Thus, it is obvious that $|\tilde{h}_p|$ follows the Rician distribution with a Rician factor $K_p =$

$|\mu_{\tilde{h}_p}|^2$, $\forall p \in [P]$, and its probability density function (pdf) is given by $p(|\tilde{h}_p|) = |\tilde{h}_p| \exp(-\frac{|\tilde{h}_p|^2}{2} - \frac{K_p}{2}) I_0(\sqrt{K_p} |\tilde{h}_p|)$, where $I_0(\cdot)$ is the modified Bessel function and $I_0(0) = 1$. Herein, $K_p = 0$, then the pdf can be simplified as $p(|\tilde{h}_p|) = |\tilde{h}_p| \exp(-\frac{|\tilde{h}_p|^2}{2})$. Note that $\hat{\mathbf{h}}$, and $\boldsymbol{\tau}$ are independent from each other. Hence, the conditional PEP dependent only on $\boldsymbol{\tau}$ and \mathbf{W} can be obtained based on the fact that $\Pr(\mathbf{q} \rightarrow \hat{\mathbf{q}}|\boldsymbol{\tau}, \mathbf{W}) = \int \Pr(\mathbf{q} \rightarrow \hat{\mathbf{q}}|\hat{\mathbf{h}}, \boldsymbol{\tau}, \mathbf{W}) p(\hat{\mathbf{h}}) d\hat{\mathbf{h}}$. Since $\{\tilde{h}_1, \dots, \tilde{h}_P\}$ are independent complex Gaussian RVs, the averaging over $|\tilde{h}_p|$ can be derived as

$$\begin{aligned} & \int_0^\infty \exp\left(-\frac{1}{4N_0} \lambda_p |\tilde{h}_p|^2\right) p(|\tilde{h}_p|) d|\tilde{h}_p| \\ &= \int_0^\infty \exp\left(-\frac{1}{4N_0} \lambda_p |\tilde{h}_p|^2\right) |\tilde{h}_p| \exp\left(-\frac{|\tilde{h}_p|^2}{2}\right) d|\tilde{h}_p| \\ &= \frac{1}{\frac{1}{2N_0} \lambda_p + 1}. \end{aligned} \quad (17)$$

Therefore, based on (17), $\Pr(\mathbf{q} \rightarrow \hat{\mathbf{q}}|\boldsymbol{\tau}, \mathbf{W})$ is given by

$$\begin{aligned} \Pr(\mathbf{q} \rightarrow \hat{\mathbf{q}}|\boldsymbol{\tau}, \mathbf{W}) &\leq \prod_{p=1}^r \frac{1}{\frac{1}{2N_0} \lambda_p + 1} \leq \prod_{p=1}^r \left(\frac{1}{2N_0} \lambda_p\right)^{-1} \\ &= \left(\frac{1}{2N_0}\right)^{-r} \left(\left(\prod_{p=1}^r \lambda_p\right)^{\frac{1}{r}}\right)^{-r}. \end{aligned} \quad (18)$$

From (18), it is evident that the performance of the considered problem depends on the rank and the geometric mean of non-zero eigenvalues, i.e., $(\prod_{p=1}^r \lambda_p)^{\frac{1}{r}}$, of the squared beamspace difference matrix. Particularly, the rank of $\mathbf{P}_{\boldsymbol{\tau}, \mathbf{W}}(\mathbf{q}, \hat{\mathbf{q}})$ determines the error exponent of the PEP (commonly referred to as the diversity gain), while its non-zero eigenvalues' geometric mean determines the SNR improvement (commonly referred to as the coding gain). These understandings align well with the conventional PEP analysis for space-time codes [18]. Therefore, a preliminary guideline for the design of the beam scheduling matrix \mathbf{W} in this problem is to maximize both the rank and the geometric mean of non-zero eigenvalues.

To access user acquisition performance, we adopt two standard metrics: missed detection rate and false alarm rate. The missed detection rate P_{MD} is the ratio between the number of missed targets in the beamspace (i.e., the sum of targets that are not detected at the correct beam direction) and number of total targets. The false alarm rate P_{FA} is the ratio between the number of mistakenly detected targets (i.e., the sum of number of detected targets minus the number of actual targets at each beam direction) and the number of total targets.

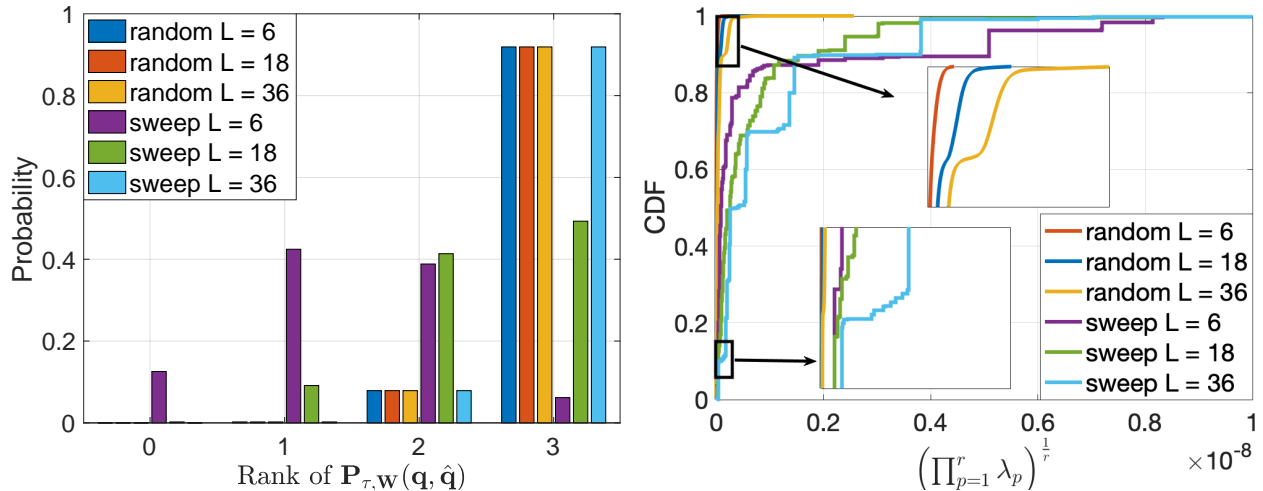


Fig. 1: Left:Evaluation on ranks. Right:Evaluation on geometric means.

V. SIMULATION RESULTS

In our simulation, we consider $M = 128$ antennas, $P = 3$ targets, bandwidth $\text{BW} = 160\text{MHz}$, the carrier frequency $f_c = 10\text{GHz}$, $N_s = 36$ subcarriers, the noise power spectral density $N_0 = -174\text{dBm/Hz}$, and the number of beam directions $N_b = 36$. In addition, for each target p , we consider the relative distance of each target is uniformly distributed between 10m and 50m, i.e., $d_p \sim \text{Unif}[10, 50]$, the radar cross section $\sigma_{p,\text{rcs}} = 20 \text{ dBsm}$, and we also assume that the AoA is uniformly distributed between $-\frac{\pi}{2}$ and $\frac{\pi}{2}$. The numerical results are averaged over 50 channel geometries and each with 100 channel realizations. To shed the light on the system design, we will provide quantitative comparisons of the two beam probing strategies provided in Section III.

A. Evaluation for the Squared Beamspace Difference Matrix

Based on the analysis in Section IV, we conduct a comparative evaluation of the two proposed beam probing strategies in terms of the rank and the geometric mean of non-zero eigenvalues for $L = \{6, 18, 36\}$ in Fig. 1. The evaluation is conducted over 50 instances of true beamspace vectors \mathbf{q} and all the possible distorted beamspace vectors. As shown in Fig. 1, we observe that the probability distribution of ranks for the random multi-beam strategy remains relatively consistent across different values of L . On the other hand, for the beam sweeping strategy, the probability on the high rank increases as time slots increase. This behavior is attributed to the

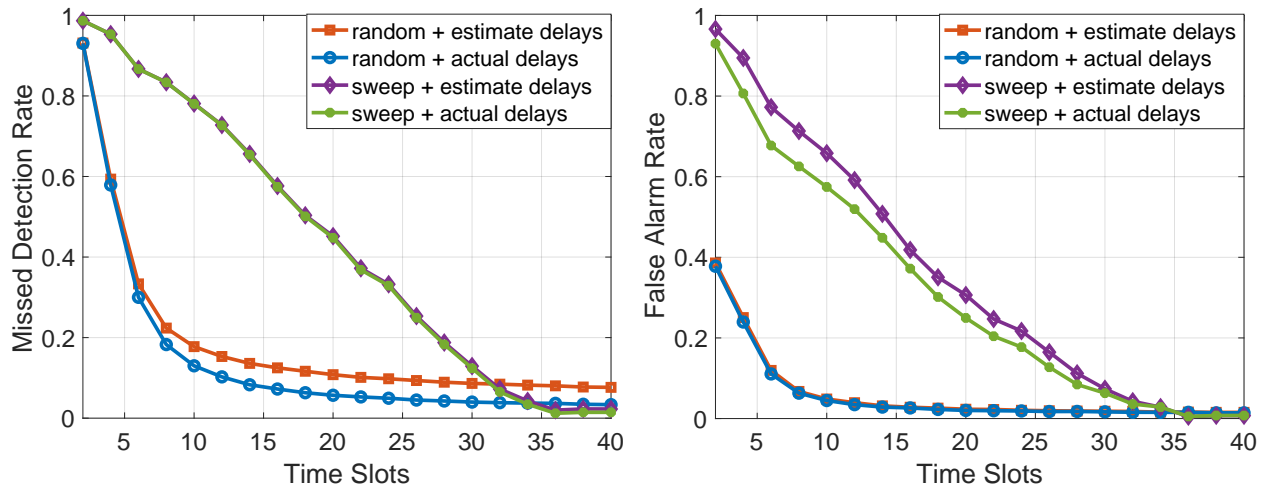


Fig. 2: Left: Evaluation on missed detection. Right: Evaluation on false alarm.

fact that the beam sweep strategy is unlikely to prob the signal to the desired direction within a short period of time. Consequently, $(\mathbf{q}_i - \hat{\mathbf{q}}_i)^T \mathbf{w}_l^s, \forall l \in [L]$, are all equal to zero, leading to a decrease in the rank of the squared beamspace difference matrix. Furthermore, we notice that the ranks corresponding to the two probing strategies converge to the same value when $L = 36$. The above observations suggest that the random multi-beam strategy enables a quick decay of the error performance compared to the beam sweeping strategy when the available time slots are less. However, when the system operates with sufficient time slots, the slopes of error curves of these two strategy are roughly the same.

We demonstrate the geometric mean of non-zero eigenvalues of the squared beamspace difference matrices corresponding to the two beam probing strategies in Fig. 1, where the beam sweeping strategy generally enjoys a larger value compared to the random multi-beam counterpart. Notice that the improvement of geometric mean of non-zero eigenvalues corresponds to the potential SNR improvement when the number of time slots available is sufficiently large. This observation indicates a superior error performance shall be observed for the beam sweeping strategy given a sufficient number of time slots, e.g., $L \geq 36$.

B. Missed detection rate and false alarm rate vs. time slots

In Fig. 2, we show the comparison between the two beam probing strategies using the proposed two-stage method. As a performance benchmark, we also plot the error performance of the

LASSO by assuming the actual delay of the users are known in prior, which serves as a lower bound for the proposed two-stage method. We observe that the random multi-beam strategy enjoys a better missed detection rate compared to the beam sweeping strategy with less number of time slots. However, the beam sweeping strategy outperforms the random multi-beam strategy when the number of time slots is sufficiently large, e.g., $L \geq 36$. These observations agree with the insights we obtained from the evaluations of the squared beamspace difference matrix. Furthermore, we also notice that the two-stage method performs general well, whose performance approaches to the results with known actual delay. We observe similar results from the false alarm rate results in Fig. 2. Specifically, we observe that the random multi-beam strategy enjoys a superior performance with less time slots but suffers performance loss with sufficiently large time slots compared to the beam sweeping strategy. Based on the above discussions, we conclude that the random multi-beam strategy is favorable when the size of the beamspace matrix is larger than the available time slots. On the other hand, the beam sweeping strategy is a better choice for beamspace matrix with a relatively small size.

VI. CONCLUSION

In this work, we focused on radar-assisted user acquisition for downlink transmissions in multi-user MIMO OFDM systems. We first proposed a two-stage method that includes the initial estimation of the delays using the MUSIC algorithm, followed by the user acquisition through the estimation of the beam space responses using a compressed sensing method. Furthermore, we conducted theoretical performance analysis based on the pairwise error probability framework, which unveils important design criteria for beam probing. Our numerical results align with our analysis and verify the effectiveness of the proposed two-stage method.

REFERENCES

- [1] F. Liu, C. Masouros, A. P. Petropulu, H. Griffiths, and L. Hanzo, "Joint radar and communication design: Applications, state-of-the-art, and the road ahead," *IEEE Trans. Commun.*, vol. 68, no. 6, pp. 3834–3862, Jun. 2020.
- [2] W. Yuan, Z. Wei, S. Li, J. Yuan, and D. W. K. Ng, "Integrated sensing and communication-assisted orthogonal time frequency space transmission for vehicular networks," *IEEE J. Sel. Top. Signal Process.*, vol. 15, no. 6, pp. 1515–1528, Nov. 2021.
- [3] T. Wild, V. Braun, and H. Viswanathan, "Joint design of communication and sensing for beyond 5G and 6G systems," *IEEE Access*, vol. 9, pp. 30 845–30 857, 2021.

- [4] F. Liu, Y. Cui, C. Masouros, J. Xu, T. X. Han, Y. C. Eldar, and S. Buzzi, "Integrated sensing and communications: Towards dual-functional wireless networks for 6G and beyond," *IEEE J. Sel. Area Commun.*, Mar. 2022.
- [5] M. Kobayashi, G. Caire, and G. Kramer, "Joint state sensing and communication: Optimal tradeoff for a memoryless case," in *Proc. IEEE Int. Symp. Inf. Theory (ISIT)*, Jun. 2018, pp. 111–115.
- [6] M. Kobayashi, H. Hamad, G. Kramer, and G. Caire, "Joint state sensing and communication over memoryless multiple access channels," in *Proc. IEEE Int. Symp. Inf. Theory (ISIT)*, Jul. 2019, pp. 270–274.
- [7] M. Ahmadipour, M. Kobayashi, M. Wigger, and G. Caire, "An information-theoretic approach to joint sensing and communication," *IEEE Trans. Inf. Theory, early access*, May 2022.
- [8] S. Li and G. Caire, "On the capacity and state estimation error of "beam-pointing" channels: The binary case," *IEEE Trans. Inf. Theory*, vol. 69, no. 9, p. 5752–5770, Sep. 2023.
- [9] C. De Alwis, A. Kalla, Q.-V. Pham, P. Kumar, K. Dev, W.-J. Hwang, and M. Liyanage, "Survey on 6G frontiers: Trends, applications, requirements, technologies and future research," *IEEE Open J. Commun. Soc.*, vol. 2, pp. 836–886, Apr. 2021.
- [10] S.-E. Chiu, N. Ronquillo, and T. Javidi, "Active learning and csi acquisition for mmwave initial alignment," *IEEE J. Sel. Areas Commun.*, vol. 37, no. 11, pp. 2474–2489, Nov. 2019.
- [11] R. Liu, M. Jian, D. Chen, X. Lin, Y. Cheng, W. Cheng, and S. Chen, "Integrated sensing and communication based outdoor multi-target detection, tracking and localization in practical 5G networks," *arXiv preprint, arXiv:2305.13924*, 2023.
- [12] S. Li, W. Yuan, C. Liu, Z. Wei, J. Yuan, B. Bai, and D. W. K. Ng, "A novel ISAC transmission framework based on spatially-spread orthogonal time frequency space modulation," *IEEE J. Sel. Areas Commun.*, vol. 40, no. 6, pp. 1854–1872, Jun. 2022.
- [13] X. Rao and V. K. Lau, "Distributed compressive CSIT estimation and feedback for FDD multi-user massive MIMO systems," *IEEE Trans. Signal Process.*, vol. 62, no. 12, pp. 3261–3271, Jun. 2014.
- [14] M. B. Khalilsarai, Y. Song, T. Yang, and G. Caire, "Fdd massive mimo channel training: Optimal rate-distortion bounds and the spectral efficiency of "one-shot" schemes," *IEEE Trans. Wireless Commun.*, vol. 22, no. 9, pp. 6018–6032, Sep. 2023.
- [15] M. A. Richards, *Fundamentals of Radar Signal Processing*. McGraw-Hill, 2014.
- [16] S. K. Dehkordi, L. Gaudio, M. Kobayashi, G. Caire, and G. Colavolpe, "Beam-space MIMO radar for joint communication and sensing with OTFS modulation," *IEEE Trans. Wireless Commun.*, vol. 22, no. 10, pp. 6737–6749, Nov. 2023.
- [17] S. Li, J. Yuan, W. Yuan, Z. Wei, B. Bai, and D. W. K. Ng, "Performance analysis of coded OTFS systems over high-mobility channels," *IEEE Trans. Wireless Commun.*, vol. 20, no. 9, pp. 6033–6048, Sep. 2021.
- [18] V. Tarokh, N. Seshadri, and A. Calderbank, "Space-time codes for high data rate wireless communication: performance criterion and code construction," *IEEE Trans. Inf. Theory*, vol. 44, no. 2, pp. 744–765, Mar. 1998.